Journal of Statistical Modelling: Theory and Applications
pp. 1-20
Yazd University Press —

JSMTA

Research Paper

Two-terminal reliability of Markov-dependent directed polyomino-chain networks and its relation to the Gutman index

Laila Azami and Nader Jafari Rad*
Department of Mathematics, Shahed University, Tehran, Iran

Received: August 09, 2026/ Revised: October 15, 2026/ Accepted: October 31, 2026

Abstract: This paper introduces an exact two-terminal reliability framework for communication networks whose topologies are modeled by directed polyomino chains. Here, "directed" specifies the prescribed growth and attachment convention; communication links themselves are undirected. The skeleton graph of a polyomino chain is interpreted as a modular communication network, in which vertices represent communication nodes and edges represent links subject to independent failures. Two boundary interfaces are used to define the source and destination terminals. For a fixed directed attachment sequence, the two-terminal reliability is defined as the probability that the source and destination remain connected after random link failures. To compute this quantity for arbitrary chain lengths, we develop a finite transfer-matrix method based on the connectivity partition of the source and the three active boundary vertices of the terminal square. Separate transfer matrices are constructed for linear and kink attachments. This approach avoids exhaustive enumeration of all link-failure configurations and yields exact reliability polynomials for deterministic directed polyomino chains. We further consider random network topologies generated by a stationary two-state Markov attachment process. A block-matrix representation is derived for the mean two-terminal reliability, incorporating both the dependence in the geometric growth of the chain and the independent failures of communication links. In addition, the Gutman index of the original polyomino-chain graph is considered as a structural descriptor of the network topology. Rather than assuming an a priori monotone relation between the Gutman index and communication reliability, the proposed framework enables their exact comparison within directed polyomino chains. The resulting model provides a mathematically tractable setting for studying the interplay between topological structure, dependent network geometry, and reliability performance.

Keywords: Communication networks; Directed polyomino chains; Gutman index; Markov-dependent random networks; Transfer matrix; Two-terminal reliability.
Mathematics Subject Classification (2010): 05C12, 05C80, 05C92.

*Corresponding author: n.jafarirad@gmail.com

1 Introduction

Topological indices are numerical graph invariants that encode structural features of molecular graphs and related discrete models. The Wiener index is one of the earliest distance-based indices, and the Gutman index combines vertex degrees with graph distances (Wiener, 1947; Dobrynin and Kochetova, 1994; Gutman, 1994; Sigarreta and Cruz-Suárez, 2024). Such indices have become standard tools in mathematical chemistry and in the structural analysis of recursively defined graph families.

Polyomino chains form a natural class of planar graphs obtained from edge-adjacent unit squares whose square-adjacency graph is a path. Their recursive construction makes them suitable for exact calculations of structural descriptors. A broad range of topological indices has been studied for deterministic polyomino chains (Ali et al., 2016; Deng et al., 2014; Golomb, 1994; Yarahmadi et al., 2012), including the Gutman index (Azami and Jafari Rad, 2025). Random polyomino-chain models have also been used to investigate expected values, variances, and asymptotic behavior of topological indices (Sigarreta et al., 2022). In particular, Markov-chain methods have been introduced for random polyomino chains in the study of Zagreb connection indices (Sigarreta and Cruz-Suárez, 2024).

Network reliability supplies a complementary probabilistic viewpoint. Given a network graph with distinguished terminals s and t, its two-terminal reliability is the probability that the operational subgraph contains an s–t path. This quantity is fundamental in the analysis of communication networks, but exact computation is generally difficult because the number of possible link states grows exponentially with the number of edges (Ball, 1986; Colbourn, 1987). For recursively constructed networks, finite-state and transfer-matrix methods provide an effective route to exact reliability polynomials (Tanguy, 2007).

The present model is also motivated by modular communication and sensor network layouts, where preserving an end-to-end connection in the presence of link failures is a basic performance requirement. In such applications, the graph should be viewed as an abstraction of a corridor-like or modular layout rather than as a literal geometric representation of a physical installation (Akyildiz et al., 2002).

In this paper, we interpret the skeleton graph of a directed polyomino chain as the topology of a communication network. Throughout, "directed" refers only to the orientation of the growth/attachment rule, not to directed communication arcs. The corners of the unit squares serve as communication nodes, and the skeleton edges serve as links subject to independent failures. Two boundary interfaces define the source and destination terminals. The chain geometry is generated by a directed linear/kink growth rule, and the sequence of attachment types is allowed to follow a stationary two-state Markov chain.

Existing polyomino-chain index studies characterize deterministic or random structural descriptors, whereas standard network-reliability methods evaluate connectivity under component failures. The distinguishing feature here is the *joint* treatment of Markov-dependent chain geometry, undirected independent link failures, and prescribed input/output interfaces. In particular, the method retains a 15-state source–boundary partition, combines it with a two-state attachment process, and gives exact comparisons with the Gutman index within this specifically defined network family; it does not assert a universal connection between reliability and that index.

The contributions of this paper are as follows. First, we formulate the corresponding two-terminal reliability problem for deterministic directed polyomino chains. Second, we develop a finite boundary-state transfer method for calculating exact reliability polynomials. Third, we incorporate Markov-dependent topology generation into a block-matrix recursion for mean two-terminal reliability. Finally, we compare this reliability measure with the Gutman index of the underlying polyomino-chain graph. No monotone relation between these two quantities is assumed a priori; rather, their relationship is examined within the present family of networks.

The remainder of the paper is organized as follows. Section 2 defines the network model and the two-terminal reliability problem. Section 3 gives exact calculations for the smallest chains. Section 4 develops the transfer matrix framework, and Section 5 incorporates Markov-dependent attachment types and exact comparisons. Section 6 provides symbolic verification and selected finite examples. The paper concludes in Section 7 with a discussion of the main findings and possible extensions.

2 Network model and two-terminal reliability

2.1 Directed polyomino chains

Let G_n be a polyomino chain consisting of n unit squares $H_1, H_2, \ldots, H_n$, where consecutive squares share exactly one edge and the adjacency graph of the squares is a path. We take G_2 to be the chain formed by two edge-adjacent unit squares.

For every $k \geq 2$, the terminal square H_k has two distinguished exposed edges. The edge $e_k^{(0)}$ is associated with a linear extension, whereas $e_k^{(1)}$ is associated with a kink extension. For $k \geq 3$, let $\eta_k \in \{0, 1\}$ denote the type of the attachment producing H_k, where

$$\eta_k = \begin{cases} 0, & \text{if the attachment is linear,} \\ 1, & \text{if the attachment is a kink.} \end{cases}$$

We impose the following non-return convention. When the square H_{k+1} is attached to the partial chain G_k across the selected edge $e_k^{(\eta_{k+1})}$, it has no other point in common with the already constructed polyomino; that is,

$$H_{k+1} \cap \bigcup_{j=1}^{k} H_j = e_k^{(\eta_{k+1})}.$$

The distinguished exposed edges are updated according to the directed growth convention: after a linear attachment, the linear and kink directions are preserved; after a kink attachment, the previous kink direction becomes the new linear direction, whereas the previous linear direction becomes the new kink direction. Under the non-return convention, the attachment sequence $\boldsymbol{\eta} = (\eta_3, \eta_4, \ldots, \eta_n)$, determines G_n uniquely up to a rigid motion of the square lattice.

We regard G_n as its skeleton graph. Hence, the vertices of G_n are the lattice corners of the squares and the edges of G_n are the unit segments belonging to the squares. The non-return condition implies that each new square contributes exactly two vertices and three edges. Thus, $|V(G_n)| = 2n + 2$, $|E(G_n)| = 3n + 1$.

2.2 Communication-network interpretation

We interpret the skeleton graph of G_n as the topology of a modular communication network. Its vertices represent communication nodes or sensors, and its edges represent communication links. Here and throughout, the adjective *directed* refers to the growth convention and to the designated linear and kink extension edges; all communication links are undirected for the purpose of two-terminal connectivity.

Let $e_{\text{in}} = \{u_0, v_0\}$, be the exposed edge of H_1 opposite to the common edge of H_1 and H_2. This edge is called the input interface. The output interface is defined to be the linear exposed edge of the terminal square:

$$e_{\text{out}} = e_n^{(0)} = \{u_n, v_n\}.$$

To define the source and destination unambiguously, we introduce two auxiliary vertices s and t. The source s is joined to u_0 and v_0, and the destination t is joined to u_n and v_n. These four auxiliary edges are assumed to be perfectly reliable. They only specify the two boundary terminals and are not regarded as random communication links.

The operational-edge set is $\mathcal{E}_n = E(G_n) \setminus \{e_{\text{in}}, e_{\text{out}}\}$. Hence, $|\mathcal{E}_n| = 3n - 1$. The augmented network is

$$\mathcal{N}_n = (V(G_n) \cup \{s, t\}, \mathcal{E}_n \cup \{su_0, sv_0, tu_n, tv_n\}) .$$

Because s and t are joined perfectly to both endpoints of their respective interfaces, deleting e_{in} and e_{out} (as above) or retaining either one as a perfectly reliable edge gives the same s–t connectivity event. We exclude these two interface edges in order to keep the random-link set equal to $\mathcal{E}_n$.

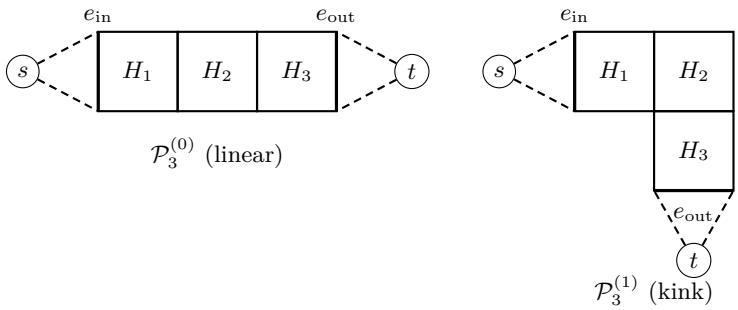


Figure 1: The terminal convention for the two directed three-square polyomino-chain networks. Solid lines are skeleton edges; the thick edges are the input and output interfaces, which are excluded from the random-link set. Dashed lines are the perfectly reliable auxiliary terminal links.

2.3 Independent edge failures

In the first version of the model, all communication nodes are assumed to function perfectly, while the operational links may fail independently. For every $e \in \mathcal{E}_n$, let

$$Y_e = \begin{cases} 1, & \text{if the link } e \text{ is operational,} \\ 0, & \text{if the link } e \text{ has failed.} \end{cases}$$

We assume that $\mathbb{P}(Y_e = 1) = r$ and $\mathbb{P}(Y_e = 0) = 1 - r$, for $0 \leq r \leq 1$, and that the random variables $\{Y_e : e \in \mathcal{E}_n\}$ are mutually independent. For a fixed attachment sequence $\boldsymbol{\eta}$, let $R_{\boldsymbol{\eta}}(r)$ denote the two-terminal reliability of the corresponding network. Thus,

$$R_{\boldsymbol{\eta}}(r) = \mathbb{P}(s \leftrightarrow t),$$

where $s \leftrightarrow t$ means that the surviving network contains at least one operational path from s to t. Equivalently,

$$R_{\boldsymbol{\eta}}(r) = \sum_{\substack{F \subseteq \mathcal{E}_n \\ s \leftrightarrow t \text{ in } \mathcal{N}_n[F]}} r^{|F|}(1-r)^{|\mathcal{E}_n|-|F|},$$

where $\mathcal{N}_n[F]$ is obtained from $\mathcal{N}_n$ by retaining precisely the operational edges in F, together with the four perfectly reliable auxiliary edges.

Remark 2.1. *The present paper considers an edge-reliability model. In particular, the simultaneous failure of all four sides of an internal square is already included as a joint realization of the independent edge-failure variables. However, squares themselves are not treated as failure-prone modules, and communication nodes are assumed to function perfectly. A correlated square- or module-failure model is a separate extension.*

2.4 Markov-generated network topologies

We now allow the shape of the polyomino chain itself to be random. Assume that $(\eta_k)_{k\geq 3}$ is a stationary two-state Markov chain with transition probabilities

$$\mathbb{P}(\eta_{k+1} = 1 \mid \eta_k = 0) = b, \qquad \mathbb{P}(\eta_{k+1} = 1 \mid \eta_k = 1) = a,$$

where $0 < a, b < 1$. Its transition matrix, with state order $0, 1$, is

$$Q = \begin{pmatrix} 1-b & b \\ 1-a & a \end{pmatrix}.$$

The stationary probabilities are $\pi_0 = \frac{1-a}{1-a+b}$, $\pi_1 = \frac{b}{1-a+b}$. The main reliability quantity in this paper is the mean two-terminal reliability $\overline{R}_n(a, b; r) = \mathbb{E}_{\boldsymbol{\eta}}\left[R_{\boldsymbol{\eta}}(r)\right]$. This expectation is taken with respect to the random topology generated by the Markov attachment process, whereas the parameter r describes the independent reliability of each operational communication link.

2.5 Gutman index as a structural descriptor

For each deterministic realization $G_n(\boldsymbol{\eta})$, write $d_{G_n}(u)$ for the number of edges incident with vertex u, and $d_{G_n}(u, v)$ for the shortest-path distance between u and v in the connected skeleton graph. Its Gutman index is

$$\mathrm{Gut}(G_n) = \sum_{\{u,v\} \subseteq V(G_n)} d_{G_n}(u) d_{G_n}(v) d_{G_n}(u, v).$$

The Gutman index is evaluated on the original polyomino-chain graph, before any communication-link failures occur. It is therefore a structural descriptor of the network

layout, whereas $R_{\boldsymbol{\eta}}(r)$ measures the probability of successful communication between the two terminals after random link failures. Accordingly, the purpose of this paper is not to assume a monotone relation between these two quantities. Instead, we investigate their relationship within directed polyomino chains and identify situations in which network layouts with different Gutman indices exhibit different two-terminal reliability values.

3 Exact calculations for small chains

In this section, we derive exact two-terminal reliability polynomials for the smallest directed polyomino chains. These examples serve two purposes. First, they validate the network model introduced in the previous section. Second, they show that the Gutman index is not, in general, a monotone predictor of two-terminal reliability, even within the family of directed polyomino chains. For a deterministic polyomino chain $\mathcal{P}$, let $A_{\mathcal{P},k}$, denote the number of operational-edge subsets of cardinality k for which the corresponding augmented network contains an operational path from s to t. If $\mathcal{P}$ has m operational edges, then

$$R_{\mathcal{P}}(r) = \sum_{k=0}^{m} A_{\mathcal{P},k} r^k (1-r)^{m-k}.$$

3.1 The two-square chain

Let $\mathcal{P}_2$ be the chain consisting of two edge-adjacent unit squares. Its skeleton graph has six vertices and seven edges. After removing the input and output interface edges from the random-link set, the network has five operational links.

Proposition 3.1. *For the two-square polyomino chain $\mathcal{P}_2$, we have*

$$\mathrm{Gut}(G(\mathcal{P}_2)) = 129 \quad \text{and} \quad R_{\mathcal{P}_2}(r) = 2r^2 + 2r^3 - 5r^4 + 2r^5.$$

Proof. The degree-distance contributions to the Gutman index are given in the following table.

$(\deg(u), \deg(v))$	$d(u,v)$	Number of pairs	Contribution
$(2,2)$	1	2	8
$(2,2)$	2	2	16
$(2,2)$	3	2	24
$(2,3)$	1	4	24
$(2,3)$	2	4	48
$(3,3)$	1	1	9

Hence,

$$\mathrm{Gut}(G(\mathcal{P}_2)) = 8 + 16 + 24 + 24 + 48 + 9 = 129.$$

For the reliability calculation, view the two squares as a horizontal row. Label the upper horizontal links of the first and second squares by a and b, respectively; label the corresponding lower horizontal links by c and d; and denote their common interior edge by h. If h fails, the network remains connected precisely when at least one of the

two independent paths (a, b) or (c, d), is operational. Therefore, $R_0 = 1 - (1 - r^2)^2 = 2r^2 - r^4$. If h is operational, it is sufficient that at least one of a, c is operational and at least one of b, d is operational. Thus, $R_1 = \left(1 - (1 - r)^2\right)^2 = (2r - r^2)^2$. Using the law of total probability with respect to the state of h, we obtain

$$\begin{aligned} R_{\mathcal{P}_2}(r) &= (1 - r)R_0 + rR_1 \\ &= (1 - r)(2r^2 - r^4) + r(2r - r^2)^2 \\ &= 2r^2 + 2r^3 - 5r^4 + 2r^5. \end{aligned}$$

□

3.2 The two directed three-square chains

Starting from $\mathcal{P}_2$, the third square may be attached either linearly or by a kink. We denote the resulting chains by $\mathcal{P}_3^{(0)}$ and $\mathcal{P}_3^{(1)}$, respectively. The superscript indicates the attachment type of the third square. The two networks are illustrated in Figure 1. Both have eight operational communication links. The exact numbers of successful operational-edge states are shown below.

Table 1: Numbers of successful operational states for the two three-square chains.

	$k=2$	$k=3$	$k=4$	$k=5$	$k=6$	$k=7$	$k=8$
$\mathcal{P}_3^{(0)}$	0	2	14	34	25	8	1
$\mathcal{P}_3^{(1)}$	1	8	25	40	26	8	1

Proposition 3.2. *For the two directed three-square polyomino chains, we have*

$$\mathrm{Gut}(G(\mathcal{P}_3^{(0)})) = 328, \qquad \mathrm{Gut}(G(\mathcal{P}_3^{(1)})) = 310.$$

Moreover,

$$\begin{aligned} R_{\mathcal{P}_3^{(0)}}(r) &= 2r^3 + 4r^4 - 2r^5 - 13r^6 + 14r^7 - 4r^8, \\ R_{\mathcal{P}_3^{(1)}}(r) &= r^2 + 2r^3 - 9r^6 + 10r^7 - 3r^8. \end{aligned}$$

Proof. A direct degree-distance enumeration in the two skeleton graphs gives

$$\mathrm{Gut}(G(\mathcal{P}_3^{(0)})) = 328, \quad \mathrm{Gut}(G(\mathcal{P}_3^{(1)})) = 310.$$

For the reliability polynomials, Table 1 lists the exact numbers $A_{\mathcal{P},k}$ of successful link states having k operational edges. Hence,

$$\begin{aligned} R_{\mathcal{P}_3^{(0)}}(r) &= 2r^3(1 - r)^5 + 14r^4(1 - r)^4 + 34r^5(1 - r)^3 \\ &\quad +25r^6(1 - r)^2 + 8r^7(1 - r) + r^8, \\ &= 2r^3 + 4r^4 - 2r^5 - 13r^6 + 14r^7 - 4r^8. \end{aligned}$$

Similarly,

$$R_{\mathcal{P}_3^{(1)}}(r) = r^2(1 - r)^6 + 8r^3(1 - r)^5 + 25r^4(1 - r)^4$$

$$
\begin{aligned}
& +40r^5(1-r)^3 + 26r^6(1-r)^2 + 8r^7(1-r) + r^8, \\
= \quad & r^2 + 2r^3 - 9r^6 + 10r^7 - 3r^8.
\end{aligned}
$$

□

Theorem 3.3. *For every* $0 < r < 1$*,*

$$\mathrm{Gut}(G(\mathcal{P}_3^{(0)})) > \mathrm{Gut}(G(\mathcal{P}_3^{(1)})),$$

whereas

$$R_{\mathcal{P}_3^{(0)}}(r) < R_{\mathcal{P}_3^{(1)}}(r).$$

Proof. The Gutman-index inequality follows from $328 > 310$. For the reliability polynomials, direct subtraction yields

$$R_{\mathcal{P}_3^{(1)}}(r) - R_{\mathcal{P}_3^{(0)}}(r) = r^2(1-r)^2(r^2 - r - 1)^2.$$

For $0 < r < 1$, we have $r^2 > 0$ and $(1-r)^2 > 0$. Moreover, $r^2 - r - 1 < 0$ on this interval, so $(r^2 - r - 1)^2 > 0$. Hence $R_{\mathcal{P}_3^{(1)}}(r) > R_{\mathcal{P}_3^{(0)}}(r)$. □

Corollary 3.4. *Within the family of directed polyomino-chain networks, the Gutman index does not induce the same ordering as two-terminal reliability.*

Proof. The two three-square chains $\mathcal{P}_3^{(0)}$ and $\mathcal{P}_3^{(1)}$ have opposite strict orderings in the preceding theorem. □

4 A transfer-matrix method

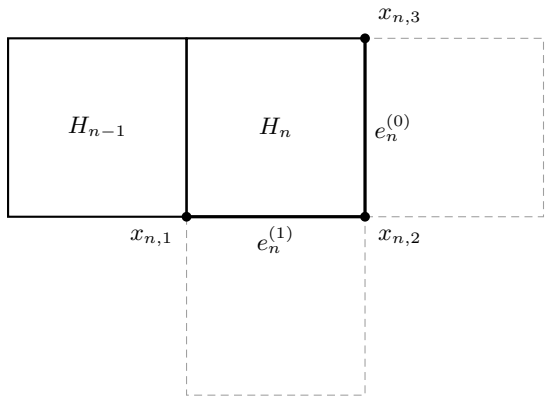


Figure 2: The active boundary of the terminal square H_n in a directed polyomino chain. The three boundary vertices are $B_n = (x_{n,1}, x_{n,2}, x_{n,3})$, where $e_n^{(1)} = \{x_{n,1}, x_{n,2}\}$ is the kink edge and $e_n^{(0)} = \{x_{n,2}, x_{n,3}\}$ is the linear edge.

4.1 Active boundary states

Let H_n be the terminal square of a directed polyomino chain. As shown in Figure 2, its two admissible attachment edges are $e_n^{(1)} = \{x_{n,1}, x_{n,2}\}$ and $e_n^{(0)} = \{x_{n,2}, x_{n,3}\}$. The first is the kink edge and the second is the linear edge. The ordered triple

$$B_n = (x_{n,1}, x_{n,2}, x_{n,3}),$$

is called the active boundary. Each of these vertices is a lattice corner of H_n. The fourth corner of H_n is not on either admissible attachment edge; hence it cannot interact directly with any future square.

Let s be the source terminal. For a realization of the operational edges in the part of the network constructed up to H_n, write $u \sim_n v$ when there is an operational path from u to v in this constructed subnetwork, where $u, v \in \{s, x_{n,1}, x_{n,2}, x_{n,3}\}$. Since $\sim_n$ is an equivalence relation, it induces a partition of this four-element set. This partition is called the boundary state at step n.

Let $\mathcal{S}$ be the set of all partitions of $\{s, x_{n,1}, x_{n,2}, x_{n,3}\}$. The complete ambient state space has cardinality equal to the fourth Bell number, $|\mathcal{S}| = B_4 = 15$. For a completely explicit matrix representation, Appendix B records the fixed ordering of these 15 partitions used in the supplementary implementation. It is essential to retain the full partition, rather than merely record which boundary vertices are connected to s. For example, the two partitions

$$\big\{\{s\}, \{x_{n,1}, x_{n,2}\}, \{x_{n,3}\}\big\} \quad \text{and} \quad \big\{\{s\}, \{x_{n,1}\}, \{x_{n,2}\}, \{x_{n,3}\}\big\},$$

have no boundary vertex connected to s, but they can evolve differently after a subsequent attachment.

Remark 4.1. *The full* 15*-state space is retained throughout the paper. This choice keeps the transition rule uniform and avoids making an a priori claim about a minimal reachable-state representation. Any state that is not reached from the initial distribution simply has probability zero, and does not affect the reliability formula.*

4.2 Boundary-separation principle

The boundary partition is sufficient because the unconstructed part of a future chain can meet the already constructed part only through the active boundary. The following statement makes this fact precise.

Lemma 4.2. *Fix a step $n \geq 2$ and a deterministic continuation of the directed polyomino chain after H_n. Consider two realizations of the operational edges in the auxiliary network constructed up to H_n. If the two realizations induce the same partition of $\{s, x_{n,1}, x_{n,2}, x_{n,3}\}$, then, for every fixed realization of all subsequently introduced random edges, the two completed networks have the same s–t connectivity status.*

Proof. By the non-return convention in Section 2, the first square added after H_n meets the already constructed polyomino precisely in its selected active boundary edge. Its only vertices belonging to $V(G_n)$ are therefore the two endpoints of that edge, which lie in B_n. Applying the same convention inductively to all subsequent squares shows that

every vertex of the future part that belongs to G_n lies in B_n. Hence the future part can meet the network constructed up to H_n only at vertices of the active boundary.

Any s–t path in a completed network can therefore be decomposed into segments contained in the constructed part and segments contained in the future part. Every segment contained in the constructed part has endpoints in $\{s, x_{n,1}, x_{n,2}, x_{n,3}\}$, and whether such a segment exists is completely determined by the corresponding block of the boundary partition. Thus, replacing one partial realization by another with the same partition cannot change the existence of an s–t path after the same future-edge configuration is attached. More formally, contract each connectivity block of the old partial network that intersects the marked set into one labelled boundary node and discard every other old component. Because no future edge has an endpoint at a discarded interior vertex, these operations preserve all possible connections among s, the new edges, and the eventual output interface. Two partial realizations with the same boundary partition therefore yield identical contracted connectivity tests for every future-edge configuration. □

4.3 Transition operators

For notational simplicity, identify $x_{n,1}, x_{n,2}, x_{n,3}$ with the labels $1, 2, 3$, respectively, and let $\sigma \in \mathcal{S}$ be a current boundary state.

For a linear attachment, the new square is attached along $e_n^{(0)} = \{x_{n,2}, x_{n,3}\}$. Let u and v be its two new vertices. The three new non-shared edges are $\alpha_0 = x_{n,2}u$, $\beta_0 = uv$,, and $\gamma_0 = vx_{n,3}$. The new active boundary is

$$B_{n+1} = (x_{n,2}, u, v).$$

For a kink attachment, the new square is attached along $e_n^{(1)} = \{x_{n,1}, x_{n,2}\}$. Its three new non-shared edges are $\alpha_1 = x_{n,1}u$, $\beta_1 = uv$,, and $\gamma_1 = vx_{n,2}$, and the directed-growth convention gives

$$B_{n+1} = (x_{n,2}, v, u).$$

For $i \in \{0, 1\}$ and $\varepsilon = (\varepsilon_1, \varepsilon_2, \varepsilon_3) \in \{0, 1\}^3$, let $\Phi_i(\sigma, \varepsilon)$ be obtained as follows:
1. add the new vertices u and v to the partition σ;
2. merge the endpoints of each new edge whose corresponding ε_j equals 1;
3. restrict the resulting connectivity relation to s and the new active boundary; and
4. relabel the new boundary vertices by $1, 2, 3$.

For $\sigma, \sigma' \in \mathcal{S}$, define

$$[T_i(r)]_{\sigma,\sigma'} = \sum_{\substack{\varepsilon \in \{0,1\}^3 \\ \Phi_i(\sigma,\varepsilon) = \sigma'}} r^{|\varepsilon|}(1-r)^{3-|\varepsilon|}.$$

Thus $T_0(r)$ and $T_1(r)$ are row-stochastic 15×15 matrices whose entries are polynomials in r. The row and column order is the explicitly listed order $S_1, \ldots, S_{15}$ in Appendix B; in particular, $S_1 = s|1|2|3$, $S_2 = s1|2|3$, $S_3 = s2|1|3$, $S_5 = s|12|3$, $S_7 = s|1|23$, $S_{14} = s|123$, and $S_{15} = s123$. The transition rule is also directly illustrated by the following representative cases:

Attachment	Initial state	New-edge states ($\varepsilon_1\varepsilon_2\varepsilon_3$)	Resulting state
linear (0)	S_1	000	S_1
linear (0)	S_1	100	S_5
linear (0)	S_1	110	S_{14}
kink (1)	S_2	000	S_1
kink (1)	S_2	100	S_4
kink (1)	S_2	110	S_{13}
kink (1)	S_2	111	S_{15}

For example, a complete row of the linear operator is

$$[T_0(r)]_{S_1,S_j} = \begin{cases} (1-r)^2, & j = 1, \\ r(1-r), & j \in \{5, 7\}, \\ r^2, & j = 14, \\ 0, & \text{otherwise.} \end{cases}$$

This follows by merging the endpoints of each operational new edge and summing the weights of all eight configurations. The supplementary implementation generates all 15 rows of each operator from this same rule, without hidden numerical parameters.

4.4 Auxiliary evolving network

For the recursive construction, the current output edge is temporarily regarded as a random edge. This is necessary because it can become an interior edge after a later attachment. The input edge is excluded from the random-link set, since the source is joined perfectly to both of its endpoints.

Lemma 4.3. *Treating the current output edge as random during the transfer calculation does not change the final two-terminal reliability.*

Proof. At the final stage the destination t is joined perfectly to both endpoints $x_{n,2}$ and $x_{n,3}$ of the output interface. If s is connected to either endpoint, then it is connected to t, regardless of whether the output edge itself is operational. If s is connected to neither endpoint, adding or deleting that edge cannot create an s–t path. Hence the event $s \leftrightarrow t$ is independent of the state of the output edge. For example, in the two-square chain G_2, take any configuration of the other five random auxiliary edges. Both endpoints of e_{out} are perfectly attached to t; changing e_{out} from failed to operational cannot alter whether s reaches t. The same argument holds at every terminal stage. If a further square is attached along the former output edge, however, that edge becomes internal and its failure state must be retained. This is why the auxiliary transfer calculation keeps the current output edge random until the final success test. □

Put $E_2^\star = E(G_2) \setminus \{e_{\text{in}}\}$. Thus, $E_2^\star$ contains the six random edges of the two-square auxiliary network, including its current output edge. For $F \subseteq E_2^\star$, let $\kappa_2(F) \in \mathcal{S}$ denote the partition of $\{s, x_{2,1}, x_{2,2}, x_{2,3}\}$ induced after declaring precisely the edges in F operational and joining s perfectly to the two endpoints of e_{in}. The initial boundary-distribution row vector $\boldsymbol{p}_2(r) = (p_{2,\sigma}(r))_{\sigma\in\mathcal{S}}$ is defined by

$$p_{2,\sigma}(r) = \sum_{\substack{F\subseteq E_2^\star \\ \kappa_2(F)=\sigma}} r^{|F|}(1-r)^{6-|F|}, \qquad \sigma \in \mathcal{S}.$$

This is an exact probability distribution, so

$$\boldsymbol{p}_2(r)\mathbf{1} = 1.$$

The formula gives a finite and fully reproducible initialization of the transfer recursion; listing all of its entries is unnecessary, since they are obtained from only $2^6 = 64$ edge states.

4.5 Reliability of a deterministic chain

For a fixed attachment word $\boldsymbol{\eta} = (\eta_3, \eta_4, \ldots, \eta_n)$, the boundary-state distribution is

$$\boldsymbol{p}_n(\boldsymbol{\eta}; r) = \boldsymbol{p}_2(r)T_{\eta_3}(r)T_{\eta_4}(r)\cdots T_{\eta_n}(r).$$

Define the column vector $\mathbf{c} = (c_\sigma)_{\sigma\in\mathcal{S}}$ by

$$c_\sigma = \begin{cases} 1, & \text{if } s \text{ is in the same block as 2 or 3 in } \sigma, \\ 0, & \text{otherwise.} \end{cases}$$

Theorem 4.4. *For every $n \geq 2$ and every deterministic directed attachment word $\boldsymbol{\eta} = (\eta_3, \ldots, \eta_n)$, the exact two-terminal reliability polynomial is*

$$R_{\boldsymbol{\eta}}(r) = \boldsymbol{p}_2(r)T_{\eta_3}(r)T_{\eta_4}(r)\cdots T_{\eta_n}(r)\mathbf{c}.$$

Proof. Lemma 4.2 shows that the boundary partition contains all information from the constructed part that can affect future s–t connectivity. At every attachment, the matrices $T_0(r)$ and $T_1(r)$ enumerate all eight states of the three newly introduced edges and update this partition exactly. Induction on the number of attachments therefore gives the displayed boundary-state distribution. At the final stage, the vector $\mathbf{c}$ selects precisely those partitions in which the source is connected to an endpoint of the output interface. Since t is joined perfectly to both endpoints of that interface, this event is equivalent to $s \leftrightarrow t$. □

5 Markov-dependent polyomino-chain networks

Assume that $(\eta_k)_{k\geq 3}$ is a stationary two-state Markov chain, where state 0 denotes a linear attachment and state 1 denotes a kink attachment. Let

$$\mathbb{P}(\eta_{k+1} = 1 \mid \eta_k = 0) = b, \qquad \mathbb{P}(\eta_{k+1} = 1 \mid \eta_k = 1) = a,$$

with transition matrix

$$Q = \begin{pmatrix} 1-b & b \\ 1-a & a \end{pmatrix}.$$

The stationary probabilities are $\pi_0 = \frac{1-a}{1-a+b}$, and $\pi_1 = \frac{b}{1-a+b}$. For $j \in \{0, 1\}$, let $\boldsymbol{w}_n^{(j)}(r)$ be the row vector whose σ-entry is the joint probability that the boundary state is σ and that $\eta_n = j$. The initialization at $n = 3$ is

$$\boldsymbol{w}_3^{(0)}(r) = \pi_0\boldsymbol{p}_2(r)T_0(r), \qquad \boldsymbol{w}_3^{(1)}(r) = \pi_1\boldsymbol{p}_2(r)T_1(r).$$

For $n \geq 3$,

$$\boldsymbol{w}_{n+1}^{(0)}(r) = \Big((1-b)\boldsymbol{w}_n^{(0)}(r) + (1-a)\boldsymbol{w}_n^{(1)}(r)\Big)\, T_0(r),$$

and

$$\boldsymbol{w}_{n+1}^{(1)}(r) = \Big(b\boldsymbol{w}_n^{(0)}(r) + a\boldsymbol{w}_n^{(1)}(r)\Big)\, T_1(r).$$

Theorem 5.1. *For every $n \geq 3$, the expected two-terminal reliability of the stationary Markov-generated network is*

$$\overline{R}_n(a,b;r) = \Big(\boldsymbol{w}_n^{(0)}(r) + \boldsymbol{w}_n^{(1)}(r)\Big)\,\mathbf{c}.$$

Proof. The two vectors retain jointly the current Markov attachment state and the boundary connectivity state. The coefficients in the two recurrences are exactly the transition probabilities of the attachment process, and the multiplication by $T_0(r)$ or $T_1(r)$ performs the corresponding connectivity update. Their sum is therefore the unconditional boundary-state distribution. Multiplication by $\mathbf{c}$ selects the successful source-to-destination states. □

5.1 Block form

Put

$$\boldsymbol{w}_n(r) = \begin{pmatrix}\boldsymbol{w}_n^{(0)}(r) & \boldsymbol{w}_n^{(1)}(r)\end{pmatrix}, \quad \mathcal{M}(a,b;r) = \begin{pmatrix}(1-b)T_0(r) & bT_1(r)\\ (1-a)T_0(r) & aT_1(r)\end{pmatrix}, \quad \mathbf{d} = \begin{pmatrix}\mathbf{c}\\ \mathbf{c}\end{pmatrix}.$$

Then, for $n \geq 3$,

$$\overline{R}_n(a,b;r) = \boldsymbol{w}_3(r)\mathcal{M}(a,b;r)^{n-3}\mathbf{d}.$$

5.2 Stationary kink frequency and persistence

Let $p = \pi_1 = \frac{b}{1-a+b}$, and $\rho = a - b$. For the stationary binary chain,

$$\mathrm{Cov}(\eta_k, \eta_{k+1}) = p(1-p)(a-b),$$

and therefore ρ is its lag-one correlation coefficient. Solving for a and b gives $a = p + (1-p)\rho$, and $b = p(1-\rho)$. Thus $\rho > 0$ represents persistence, $\rho = 0$ gives the independent Bernoulli model, and $\rho < 0$ represents a tendency to alternate. For example, if $p = 1/2$ and $\rho = 0.6$, then $a = 0.8$ and $b = 0.2$: linear attachments tend to follow linear attachments and kinks tend to follow kinks. If $p = 1/2$ and $\rho = -0.6$, then $a = 0.2$ and $b = 0.8$, so linear and kink attachments tend to alternate. Both chains have the same stationary kink frequency $p = 1/2$; only the dependence differs. For fixed $p \in (0,1)$, the admissible interval is

$$-\min\left\{\frac{p}{1-p}, \frac{1-p}{p}\right\} < \rho < 1.$$

5.3 Exact comparisons for three and four squares

For three squares, the stationary kink probability is p, and the two possible attachment words are 0 and 1. From Section 3,

$$R_1(r) - R_0(r) = r^2(1-r)^2(r^2-r-1)^2 > 0 \qquad (0 < r < 1).$$

Hence

$$\overline{R}_3(p;r) = R_0(r) + p\, r^2(1-r)^2(r^2-r-1)^2,$$

whereas

$$\mathbb{E}[\mathrm{Gut}(G_3)] = 328 - 18p.$$

Consequently, increasing the stationary kink frequency decreases the expected Gutman index but increases the mean two-terminal reliability within the three-square family.

For four squares, write $R_{ij}(r)$ for the reliability polynomial associated with the word (i, j). Exact calculations give

$$\mathrm{Gut}(G_4(00)) = 665, \quad \mathrm{Gut}(G_4(01)) = \mathrm{Gut}(G_4(10)) = 629, \quad \mathrm{Gut}(G_4(11)) = 611.$$

The stationary word probabilities are

$$\begin{aligned} \mathbb{P}(00) &= (1-p)^2 + p(1-p)\rho, \\ \mathbb{P}(01) &= \mathbb{P}(10) = p(1-p)(1-\rho), \\ \mathbb{P}(11) &= p^2 + p(1-p)\rho. \end{aligned}$$

Since $R_{01}(r) = R_{10}(r)$, it follows that

$$\begin{aligned} \overline{R}_4(p,\rho;r) = {} & \big((1-p)^2 + p(1-p)\rho\big)R_{00}(r) \\ & + 2p(1-p)(1-\rho)R_{01}(r) \\ & + \big(p^2 + p(1-p)\rho\big)R_{11}(r). \end{aligned}$$

The four-square polynomials listed in Appendix A satisfy

$$R_{00}(r) - 2R_{01}(r) + R_{11}(r) = -r^3(1-r)^3(1+r)(r^2-r-1)^2.$$

Theorem 5.2. *For every $0 < p < 1$ and $0 < r < 1$,*

$$\frac{\partial}{\partial\rho}\overline{R}_4(p,\rho;r) = -p(1-p)r^3(1-r)^3(1+r)(r^2-r-1)^2 < 0.$$

Moreover,

$$\mathbb{E}[\mathrm{Gut}(G_4)] = 665 - 72p + 18p^2 + 18p(1-p)\rho,$$

and hence

$$\frac{\partial}{\partial\rho}\mathbb{E}[\mathrm{Gut}(G_4)] = 18p(1-p) > 0.$$

Proof. Differentiate the displayed expression for $\overline{R}_4$ with respect to ρ and use the exact factorization above. The formula for the expected Gutman index follows by averaging the four displayed Gutman indices using the stationary word probabilities. □

For fixed stationary kink frequency, increased persistence has opposite effects on the expected Gutman index and the mean two-terminal reliability in the four-square family. Structurally, increasing ρ transfers probability mass from the mixed words $01, 10$ to the homogeneous words $00, 11$ while holding p fixed. The mixed-word Gutman index is 629, below the mean $(665 + 611)/2 = 638$ of the two homogeneous indices; therefore the expected Gutman index rises. Conversely, the exact identity $R_{00}(r) - 2R_{01}(r) + R_{11}(r) < 0$ shows that the mixed-word reliability exceeds the corresponding homogeneous-word average, so mean reliability falls. This mechanism concerns the four-square terminal network model studied here, not arbitrary networks.

6 Exact computational verification and illustrative examples

6.1 Exact implementation of the transfer method

The transfer matrices $T_0(r)$ and $T_1(r)$ can be constructed exactly by enumerating the eight operational configurations of the three new edges introduced at each attachment step. More precisely, for every boundary state $\sigma \in \mathcal{S}$ and every attachment type $i \in \{0, 1\}$, we consider all vectors $\varepsilon \in \{0, 1\}^3$. For each ε, the corresponding updated state $\Phi_i(\sigma, \varepsilon)$ is obtained by merging the endpoints of the operational new edges, restricting the resulting equivalence relation to the new active boundary, and relabelling the boundary vertices by $1, 2, 3$. Thus, every entry of $T_i(r)$ is computed as a finite sum of terms of the form

$$r^k(1 - r)^{3-k}, \qquad 0 \le k \le 3.$$

The initial vector $\boldsymbol{p}_2(r)$ is obtained by enumerating the operational states of the auxiliary two-square network. In this auxiliary network, the input edge is excluded from the random-link set, whereas the current output edge is temporarily retained, as explained in the previous section. All computations are carried out symbolically. Consequently, the resulting reliability polynomials have exact integer coefficients and no floating-point approximation is used in their derivation.

6.2 Verification by exhaustive enumeration

For a directed polyomino chain with n squares, the original two-terminal reliability model contains $3n - 1$ random operational links. Hence direct exhaustive enumeration examines 2^{3n-1} link-failure configurations for each fixed attachment word.

To validate the implementation of the transfer-matrix method, we compared its output with direct exhaustive enumeration for every attachment word of lengths up to five squares. Specifically, all $1 + 2 + 4 + 8 = 15$ directed attachment words with $n = 2, 3, 4, 5$ were examined. The verification counts, aggregated over all attachment words of each length, are recorded explicitly in Table 2. The calculations were reproduced with Python 3.13 and SymPy 1.14; all 15 exact symbolic polynomial comparisons passed. The finite verification requires a total of 139808 direct link configurations.

For every tested attachment word, the reliability polynomial obtained from direct enumeration coincided exactly with the polynomial obtained from the transfer-matrix

Table 2: Exact exhaustive verification by chain length. Each attachment word agrees with the corresponding transfer-matrix polynomial.

Squares n	Words	Random links/word	Configurations/word	Total checked
2	1	5	32	32
3	2	8	256	512
4	4	11	2048	8192
5	8	14	16384	131072
Total	15	–	–	139808

formula

$$R_{\boldsymbol{\eta}}(r) = \boldsymbol{p}_2(r)T_{\eta_3}(r)T_{\eta_4}(r)\cdots T_{\eta_n}(r)\mathbf{c}.$$

This finite verification is not used as a proof of the transfer-matrix theorem. The theorem follows from the boundary-state argument. The purpose of the exhaustive check is to validate the implementation and, in particular, to detect possible errors in boundary ordering, interface selection, or the kink-update convention.

6.3 Selected exact values

Table 3 presents selected exact computations. The attachment word records the successive types of attachment after the initial two-square chain, where 0 denotes a linear attachment and 1 denotes a kink attachment.

Table 3: Selected values of the Gutman index and two-terminal reliability for directed polyomino-chain networks.

n	Attachment word	$\mathrm{Gut}(G_n)$	$R_{\boldsymbol{\eta}}(1/2)$	$R_{\boldsymbol{\eta}}(0.9)$
2	$\varnothing$	129	0.500000	0.978480
3	0	328	0.328125	0.966975
3	1	310	0.425781	0.976598
4	00	665	0.214844	0.955596
4	01	629	0.278320	0.965101
4	11	611	0.305176	0.972961
5	011	1086	0.199585	0.961506
5	101	1086	0.222107	0.963073

The entries for the three-square chains agree with the exact formulas derived previously. In particular, $\mathrm{Gut}(G_3^{(0)}) = 328$, and $\mathrm{Gut}(G_3^{(1)}) = 310$, whereas $R_{G_3^{(1)}}(r) > R_{G_3^{(0)}}(r)$, $0 < r < 1$. Thus, even for chains of the same length, a larger Gutman index does not necessarily imply a larger two-terminal reliability.

6.4 Equal Gutman index and different reliability

The five-square examples in Table 3 provide a second important observation. The two attachment words 011 and 101 satisfy

$$\mathrm{Gut}(G_5(011)) = \mathrm{Gut}(G_5(101)) = 1086.$$

However, their two-terminal reliability values are different. For example, at $r = 1/2$, $R_{011}(1/2) = \frac{1635}{8192}$, whereas $R_{101}(1/2) = \frac{3639}{16384}$. Since $\frac{1635}{8192} \neq \frac{3639}{16384}$, the Gutman index

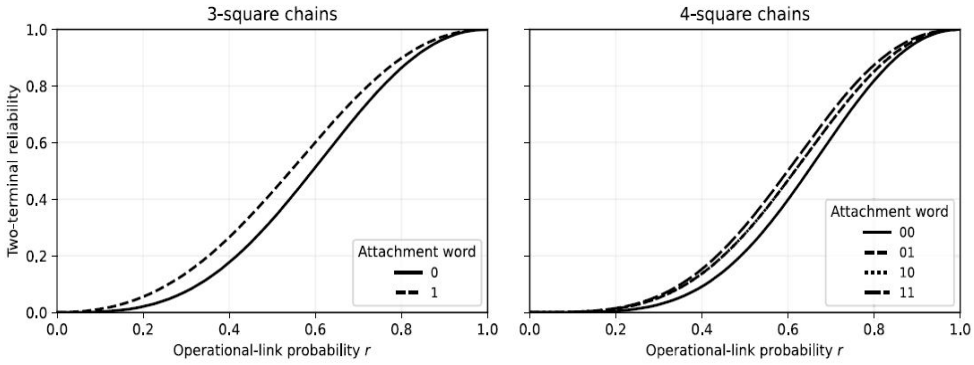


Figure 3: Exact two-terminal reliability curves as functions of the operational-link probability r for the directed three-square (left) and four-square (right) examples. The line styles identify attachment words (0: linear, 1: kink). Each curve is evaluated from the exact symbolic polynomial, without fitting.

does not uniquely determine two-terminal reliability, even when the chain length is fixed. This phenomenon arises because the Gutman index is computed from the degree-distance structure of the original skeleton graph, whereas two-terminal reliability also depends on the prescribed input and output interfaces and on the arrangement of alternative operational paths between them. Therefore, within the present network model, the Gutman index should be regarded as a structural descriptor rather than as a complete predictor of communication reliability. These comparisons depend on the specified input/output interfaces and independent-edge-failure assumptions; they are not asserted to hold for general graph families or reliability models.

7 Conclusion and future work

In this paper, we introduced a communication-network model based on directed polyomino chains. The skeleton graph of a polyomino chain was interpreted as a modular network topology, in which graph vertices represent communication nodes and graph edges represent communication links. The source and destination were attached to the endpoints of the input and output interfaces by perfectly reliable auxiliary terminal links. All remaining operational links were assumed to fail independently with probability $1 - r$. For a fixed directed attachment sequence $\boldsymbol{\eta} = (\eta_3, \eta_4, \ldots, \eta_n)$, the main quantity of interest was the two-terminal reliability $R_{\boldsymbol{\eta}}(r)$, namely, the probability that the source remains connected to the destination after random link failures. The main theoretical contribution of the paper is an exact transfer-matrix framework for the computation of $R_{\boldsymbol{\eta}}(r)$. The method is based on the connectivity partition of the source and the three active boundary vertices of the terminal square. The complete ambient state space consists of the 15 partitions of $\{s, x_{n,1}, x_{n,2}, x_{n,3}\}$. For each attachment type, namely a linear attachment and a kink attachment, a corresponding transfer matrix $T_0(r)$ or $T_1(r)$, updates the boundary connectivity distribution. As a consequence, the two-terminal reliability polynomial of every deterministic directed polyomino chain is

obtained in the form $R_{\boldsymbol{\eta}}(r) = \boldsymbol{p}_2(r)T_{\eta_3}(r)T_{\eta_4}(r)\cdots T_{\eta_n}(r)\boldsymbol{c}$. The formulation is exact for every chain length and avoids exhaustive enumeration of all link-failure configurations. Direct enumeration is still feasible for short chains and was used to verify the transfer calculation for all directed attachment words with $n = 2, 3, 4, 5$.

For every tested chain, the reliability polynomial obtained from the transfer method coincided exactly with the polynomial obtained by exhaustive enumeration. We then incorporated the Markov-dependent growth mechanism. In this model, the successive attachment types form a stationary two-state Markov chain, where state 0 represents a linear attachment and state 1 represents a kink attachment. The expected two-terminal reliability of the resulting random network can be computed through a finite block matrix recursion. More precisely, if $\boldsymbol{w}_n(r) = \begin{pmatrix}\boldsymbol{w}_n^{(0)}(r) & \boldsymbol{w}_n^{(1)}(r)\end{pmatrix}$, then $\overline{R}_n(a, b; r) = \boldsymbol{w}_3(r)\mathcal{M}(a, b; r)^{n-3}\boldsymbol{d}$. Therefore, the stochastic dependence in the geometry of the chain and the independent failures of the communication links are both included in one exact finite-dimensional framework.

A second objective of the paper was to investigate the relationship between the Gutman index and two-terminal reliability. The Gutman index was evaluated on the original skeleton graph of the polyomino chain, before link failures occur. Hence, it acts as a degree-distance descriptor of the network topology, whereas two-terminal reliability measures the probability of successful communication between the two specified boundary terminals. The exact three-square computations show that these quantities are not necessarily monotone with respect to one another. In particular, $\mathrm{Gut}(G_3^{(0)}) > \mathrm{Gut}(G_3^{(1)})$, while $R_{G_3^{(0)}}(r) < R_{G_3^{(1)}}(r)$, $0 < r < 1$. Thus, even within the restricted family of directed polyomino chains, a larger Gutman index does not necessarily imply a larger two-terminal reliability. The four-square stationary Markov family provides a further comparison. For a fixed stationary kink frequency p, the expected Gutman index is strictly increasing with respect to the persistence parameter ρ, whereas the mean two-terminal reliability is strictly decreasing with respect to ρ. Hence, in this family, increasing the tendency of equal attachment types to occur consecutively increases the expected Gutman index but decreases the expected communication reliability. Moreover, examples with five squares show that two directed polyomino chains may have the same Gutman index while having different two-terminal reliability values . Consequently, the Gutman index neither preserves the reliability ordering nor completely determines two-terminal reliability in the present network model.

The results of this paper suggest several directions for future work. One possible direction is to identify a minimal reachable-state representation and thereby reduce the dimension of the transfer matrices. Another direction is to study the asymptotic behavior of $\overline{R}_n(a, b; r)$, as the number of squares tends to infinity, using the spectral properties of the block transfer matrix. It would also be natural to extend the model by allowing node failures, non-identical link-reliability probabilities , direction-dependent communication links, or correlated failures. From an applied viewpoint, the model can be interpreted as an abstraction of a modular corridor, tunnel, or sensor-network layout in which the local geometry of the network may change according to a dependent stochastic mechanism. Finally, an interesting optimization problem is to determine, among directed polyomino chains of a fixed length, those topologies that maximize two-terminal reliability subject to structural constraints involving the Gutman index or other topological descriptors.

References

Akyildiz, I.F., Su, W., Sankarasubramaniam, Y. and Cayirci, E. (2002). Wireless sensor networks: a survey. *Computer Networks*, **38**(4):393–422.

Ali, A., Raza, Z. and Bhatti, A.A. (2016). Bond incident degree (BID) indices of polyomino chains: A unified approach. *Applied Mathematics and Computation*, **287**:28–37.

Azami, L. and Jafari Rad, N. (2025). Gutman index of polyomino chains. *Journal of Discrete Mathematics and Its Applications*, **10**(4):375–392.

Ball, M.O. (1986). Computational complexity of network reliability analysis: an overview. *IEEE Transactions on Reliability*, **35**(3):230–239.

Colbourn, C.J. (1987). *The Combinatorics of Network Reliability*. New York: Oxford University Press.

Deng, H., Balachandran, S., Ayyaswamy, S.K. and Venkatakrishnan, Y.B. (2014). The harmonic indices of polyomino chains. *National Academy Science Letters*, **37**(5):451–455.

Dobrynin, A.A. and Kochetova, A.A. (1994). Degree distance of a graph: A degree analog of the Wiener index. *Journal of Chemical Information and Computer Sciences*, **34**(5):1082–1086.

Golomb, S.W. (1994). *Polyominoes: Puzzles, Patterns, Problems, and Packings*. 2nd edition, Princeton University Press.

Gutman, I. (1994). Selected properties of the Schultz molecular topological index. *Journal of Chemical Information and Computer Sciences*, **34**(5):1087–1089.

Sigarreta, S.C., Sigarreta, S.M. and Cruz-Suárez, H. (2022). On degree-based topological indices of random polyomino chains. *Mathematical Biosciences and Engineering*, **19**(9):8760–8773.

Sigarreta, S. and Cruz-Suárez, H. (2024). Zagreb connection indices on polyomino chains and random polyomino chains. *Open Mathematics*, **22**(1):20240057.

Tanguy, C. (2007). What is the probability of connecting two points? *Journal of Physics A: Mathematical and Theoretical*, **40**(47):14099–14116.

Wiener, H. (1947). Structural determination of paraffin boiling points. *Journal of the American Chemical Society*, **69**(1):17–20.

Yarahmadi, Z., Ashrafi, A.R. and Moradi, S. (2012). Extremal polyomino chains with respect to Zagreb indices. *Applied Mathematics Letters*, **25**(2):166–171.

Appendix

Four-square reliability polynomials
For completeness, the three distinct four-square reliability polynomials used in Section 5 are

$$\begin{aligned} R_{00}(r) &= 2r^4 + 6r^5 + 2r^6 - 18r^7 - 15r^8 + 52r^9 - 36r^{10} + 8r^{11}, \\ R_{01}(r) &= r^3 + 3r^4 + 2r^5 - 3r^6 - 7r^7 - 11r^8 + 36r^9 - 26r^{10} + 6r^{11}, \\ R_{11}(r) &= r^3 + 4r^4 + 3r^5 - 10r^6 - 4r^7 - r^8 + 23r^9 - 20r^{10} + 5r^{11}. \end{aligned}$$

The word 10 has the same reliability polynomial as the word 01. A direct subtraction gives

$$R_{00}(r) - 2R_{01}(r) + R_{11}(r) = -r^3(1-r)^3(1+r)(r^2-r-1)^2,$$

which is the identity used in the proof of the four-square comparison theorem.

Boundary-state order for the transfer matrices
The transfer formula in Section 4 is independent of any ordering of the partitions in $\mathcal{S}$. For reproducibility, the supplementary code uses the following fixed order, where a vertical bar separates distinct connectivity blocks:

$$\begin{array}{lll} S_1 = s \mid 1 \mid 2 \mid 3, & S_2 = s1 \mid 2 \mid 3, & S_3 = s2 \mid 1 \mid 3, \\ S_4 = s3 \mid 1 \mid 2, & S_5 = s \mid 12 \mid 3, & S_6 = s \mid 13 \mid 2, \\ S_7 = s \mid 1 \mid 23, & S_8 = s1 \mid 23, & S_9 = s2 \mid 13, \\ S_{10} = s3 \mid 12, & S_{11} = s12 \mid 3, & S_{12} = s13 \mid 2, \\ S_{13} = s23 \mid 1, & S_{14} = s \mid 123, & S_{15} = s123. \end{array}$$

Rows and columns of the machine-generated matrices $T_0(r)$ and $T_1(r)$ are indexed by this order. The matrices themselves are generated exactly from the map Φ_i in Section 4.3 and are provided in the accompanying symbolic code.